

High-Field Magnetoresistance of IrO_2

W. D. Ryden

Bell Laboratories, Allentown, Pennsylvania 18104

and

W. A. Reed and E. S. Greiner*

Bell Laboratories, Murray Hill, New Jersey 07974

(Received 9 March 1972)

The monotonic and oscillatory magnetoresistance of IrO_2 is reported and found to be consistent with the Fermi-surface model proposed by Graebner.

I. INTRODUCTION

There is considerable interest in understanding the electronic band structure of the transition-metal oxides. In this paper we wish to report measurement of both the monotonic and oscillatory components of the magnetoresistance of IrO_2 which is one of a series of metal oxides which crystallize in the rutile structure and exhibit metallic conduction. This particular investigation was undertaken in order to further substantiate various topological features of a model of the Fermi surface proposed by Graebner¹ on the basis of his magnetothermal measurements and preliminary augmented-plane-wave (APW) band calculations by Mattheiss.²

A review of high-field magnetoresistance and the theoretical basis for its interpretation can be found in Ref. 3.

II. EXPERIMENTAL DETAILS

Single crystals of IrO_2 which have the rutile structure, were grown by a vapor-transport technique.

Oxygen was passed over metallic Ir in a quartz tube at 1100°C to form volatile IrO_3 . This was transported to a cooler part of the tube where between $(800\text{--}900)^\circ\text{C}$ it decomposed to form the IrO_2 crystals. The crystals having the highest residual resistance ratios (~ 1400) were all needles oriented along the tetragonal c axis. These crystals are ideal for four-probe resistance measurements with the current directed along the c axis. Samples having the current directed perpendicular to this axis were made by spark-cutting sections from the c -axis needles. The small size of these latter samples (~ 0.1 mm on a side) did not allow four-probe measurements.

The leads were attached to the samples by first making small "dots" of colloidal silver and then baking them at 500°C for $\frac{1}{2}$ h. Fine copper leads were then soldered to the dots using a silver-saturated PbSn solder. The samples were mounted on a holder which allowed rotation in the magnetic field⁴ and the dc measurements were made in the standard manner. To enhance the oscillatory part

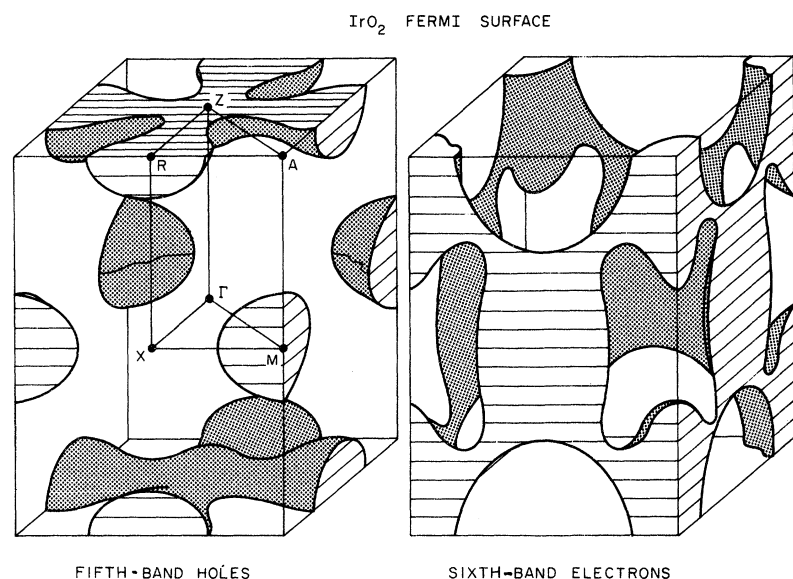


FIG. 1. Fermi surface of IrO_2 as proposed by Graebner (Ref. 1).

orbits are related to the first, but rely on degeneracy of the fifth and sixth bands along the AM and XM zone lines for their existence. The angular range of existence of these coupled open orbits should be complementary to that of the first set.

The angular range over which the $\langle 101 \rangle$ -directed orbits exist will depend on the orientation of the sixth-band necks with respect to the zone-face diagonal. The $\{101\}$ crystallographic plane is a non-symmetry plane and there is, therefore, no guarantee that this connecting piece is centered along the zone-face diagonal.⁵

The $[001]$ -, $\langle 100 \rangle$ -, and $\langle 101 \rangle$ -directed open orbits of the six-band electron surface should all degenerate to a closed-hole orbit for the field \vec{H} exactly along $\langle 100 \rangle$. The $\langle 100 \rangle$ direction should be surrounded by a two-dimensional region of open orbits of small angular extent.

IV. EXPERIMENTAL DATA AND DISCUSSION

A. Monotonic Magnetoresistance

The anisotropy of the magnetoresistance obtained at 100 kOe is shown in Figs. 2 and 3 for samples Ir 1 ($\vec{J} \parallel [001]$) and Ir 2 ($\vec{J} \parallel [0\bar{1}0]$), respectively. In Fig. 4 we show a stereogram of field directions which allow open trajectories on the Fermi surface. The lines represent one-dimensional regions of open orbits and the shaded areas are the two-dimensional regions of open orbits. We find that we can account for all of the open orbits using the Fermi-surface model proposed by Graebner.

The anisotropy resulting from the $\langle 100 \rangle$ -directed open orbits of the fifth-band-hole surface are clearly visible in Figs. 2 and 3 for rotation angles passing through the $\{100\}$ planes. The field dependence of sample Ir 1 with \vec{H} lying in the (100) plane is found to saturate with $\Delta\rho/\rho_0 \approx 6$. The field depen-

EXPANDED STEREOGRAM OF MAGNETORESISTANCE OF IrO_2

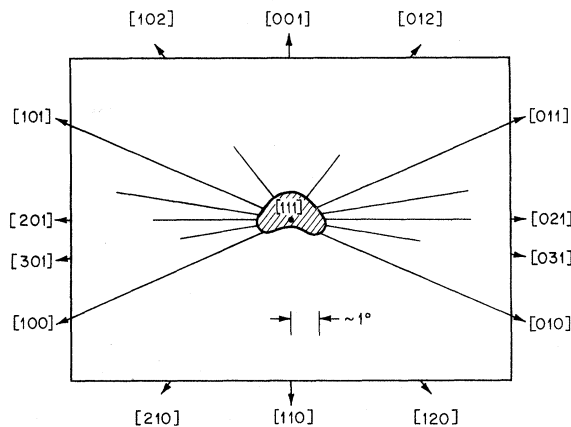


FIG. 5. Enlargement of Fig. 4 around $[111]$.

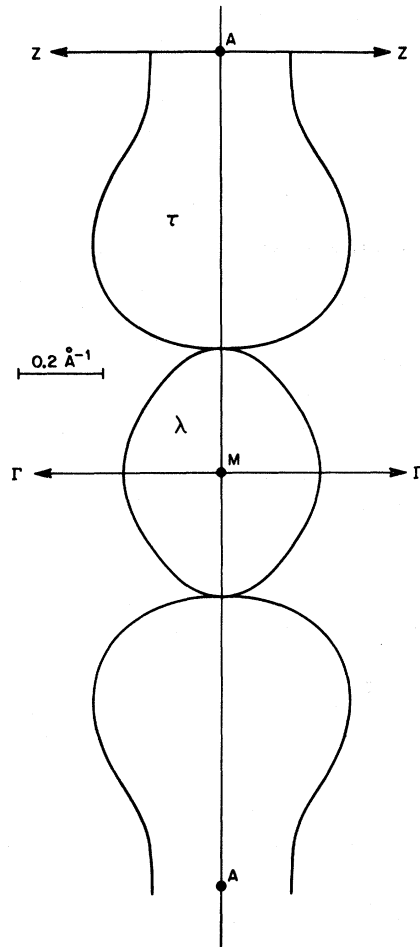


FIG. 6. Cross section of IrO_2 Fermi surface along the AM -zone line. The curves represent self-intersecting trajectories formed from the fifth- and sixth-band hole and electron surfaces, respectively. The corresponding frequencies of the electron and hole trajectories as reported by Graebner (Ref. 1) and also observed here are $\tau = 0.680 \times 10^8$ and $\lambda = 0.202 \times 10^8$ G, respectively.

dence for this sample in a general direction was found to obey a relation of the form $\rho_0 \sim H^{1.89}$, in good agreement with the behavior expected of a compensated metal.

Evidence for the $\langle 110 \rangle$ -directed orbits on this surface is seen in Fig. 2 for a rotation angle lying in the (110) plane and also in Fig. 3 as the dips labeled $c - c'$. (The anisotropy is less pronounced in the latter case since the open direction in k space is not perpendicular to the current direction as it is in the former case.) The $\langle 110 \rangle$ -directed orbits are found to exist to within a few degrees of $\langle 111 \rangle$ in the (110) plane.

The fifth-band-hole surface also supports a two-dimensional region of open orbits centered on $[001]$. This region was mapped out using both sample Ir 1,

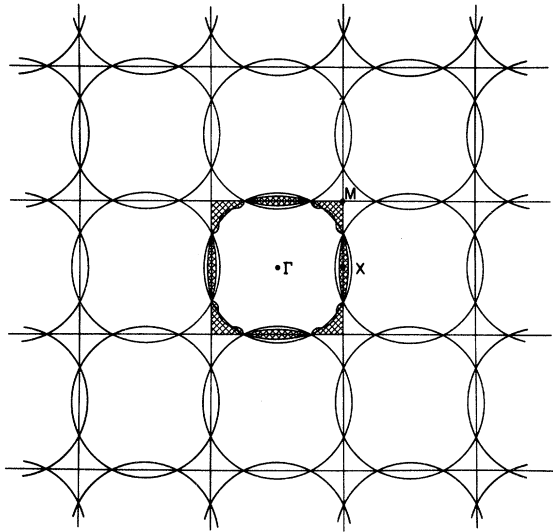


FIG. 7. (001) central cross section of the IrO_2 Fermi surface. The overlapping circles closely approximate the actual trajectories which are the perimeter of the cross-hatched areas.

and Ir 2 and is clearly shown in Fig. 4.

The anisotropy which is observed upon crossing the (001) plane for sample Ir 2 and shown in Fig. 3 has been assigned to the $[001]$ -directed open orbits on the six-band electron surface. The narrowing of the dip which occurs about 20 deg from $\langle 100 \rangle$ is thought to correspond to the transition from uncoupled to coupled orbits. Detailed field-dependence measurements across this region could confirm this difference; however, these measurements were not possible using our two-probe sample. Further evidence supporting the existence of coupled trajectories along the AM zone line will be given below.

The existence of the $\langle 100 \rangle$ -directed open orbits on the sixth-band electron surface is not readily apparent from our data. The reason for this is presumably attributable to the simultaneous existence of a much larger band of $\langle 100 \rangle$ open orbits on the fifth-band-hole surface. The existence of the two-dimensional region of open orbits about $\langle 100 \rangle$ is also not clear. However, the additional broadening of the (001) plane dip of Fig. 3 near $\langle 100 \rangle$ ($\Phi' \lesssim 5^\circ$) as well as the extra structure visible there is consistent with a two-dimensional region about $\langle 100 \rangle$. Our estimate of the angular extent of this region based on our data is shown in Fig. 4 by the dashed perimeter surrounding $\langle 100 \rangle$.

As discussed above, the sixth-band electron surface is also thought to support open trajectories along the zone-face diagonals. The angular range

over which such orbits exist is not obvious from the Fermi-surface model, but it is readily apparent from our data that these orbits exist over the entire $\{101\}$ plane. In the case of sample Ir 2 with the current along $[0\bar{1}0]$ there are, in terms of the magnetoresistance behavior, two inequivalent $\{101\}$ planes. For the field in the $(\bar{1}01)$ plane, the open direction in k space, $[101]$, is perpendicular to the current direction and the magnetoresistance must saturate. On the other hand, for the field in the (011) plane the open direction in k space, $[011]$, is not perpendicular to the current direction and the magnetoresistance must vary quadratically with field resulting in somewhat less anisotropy. Quantitative agreement with the above field dependences cannot be obtained due to the two-probe measurements on sample Ir 2. However, the expected qualitative difference in the anisotropy resulting from the $[\bar{1}01]$ and $[011]$ open orbits is observed and is shown in Fig. 3 at rotations labeled a and b through b' , respectively.

The broadening of the dip in the magnetoresistance occurring at $\Phi' = 40^\circ$ for the $\langle 101 \rangle$ -type open orbits corresponds to crystallographic $\langle 111 \rangle$ directions and is indicative of a two-dimensional region centered at $\langle 111 \rangle$. This region is of small angular extent and has been mapped out by examining the magnetoresistance anisotropy for a large number of closely spaced rotations passing near $\langle 111 \rangle$. This region is shown in more detail in Fig. 5.

B. Oscillatory Magnetoresistance

Further evidence supporting the model of Fig. 1 is obtained from our oscillatory data. These data are

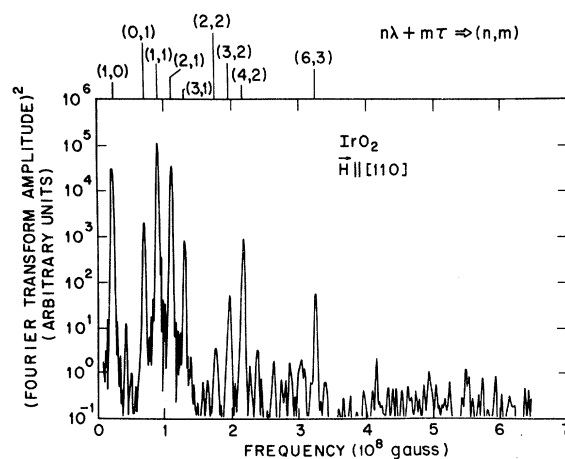


FIG. 8. Frequency components of oscillatory magnetoresistance for magnetic field along $[110]$. This spectrum corresponds to the case of self-intersecting trajectories shown in Fig. 6. The observed components of the spectrum are labeled (n, m) denoting the frequency values $n\lambda + m\tau$, where the values of λ and τ are given in Fig. 6.

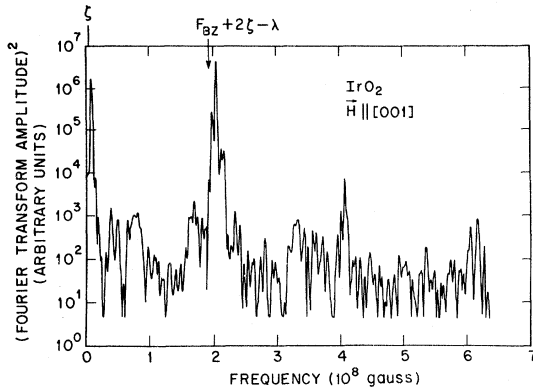


FIG. 9. Frequency components of oscillatory magnetoresistance for magnetic field along [001]. This spectrum corresponds to the case of overlapping trajectories shown in Fig. 7. The labeled frequencies are discussed in the text.

taken over angular regions for which coupled trajectories between the fifth- and sixth-band surfaces exist. These trajectories result from symmetry-induced band degeneracies along the XM and AM zone lines.⁵ It follows from these considerations that the closed fifth-band-hole surface must contact the sixth-band electron surface along both the XM and AM symmetry directions. Under these conditions the model will support several coupled trajectories. In particular there will be an open trajectory centered along the ([001] directed) AM zone line. This trajectory is of the self-intersecting type and its cross section is shown in Fig. 6. For the field along [001] there will also exist a two-dimensional network of closed trajectories as shown in Fig. 7. Tipping the field away from [001] in a {100} plane will result in this network transforming into a set of self-intersecting trajectories along <100> directions. In the case of self-intersecting trajectories we have found in several other metals the existence of relatively large magnetoresistance oscillations of peculiar spectral character.⁶ These oscillations are composed of the frequency components corresponding to the uncoupled

orbits of the linear chain plus a large number of components which are only the sums of the uncoupled components. The spectrum which we find in the case of Fig. 6 is consistent with this description and is shown in Fig. 8. It should be pointed out that the observed frequencies *do not* correspond to extended closed orbits on the chain, and these latter frequency components are systematically absent. This unexpected distribution of frequency components will be discussed further in Ref. 7.

For the field oriented along the [001] axis, we observe large amplitude oscillations, the larger components of which fall within a manifold containing the frequency expected for the overlapping closed orbits shown schematically in Fig. 7. This spectrum is shown in Fig. 9. The lowest component ζ corresponds to the frequency assigned by Graebner to the X -centered pancake. The frequency λ corresponding to the M -centered hole surface is not observed here. We have, however, used Graebner's measured value of λ to calculate the giant-orbit frequency which is given by $F_{BZ} + 2\zeta - \lambda$, where $F_{BZ} = 2.05 \times 10^8$ G is derived from the (001) Brillouin zone (BZ) area, $\zeta = 0.0615 \times 10^8$ G, and $\lambda = 0.222 \times 10^8$ G.

The dominant frequencies of the manifold are 1.97×10^8 and 2.04×10^8 G. The calculated giant-orbit frequency is 1.95×10^8 G, and is within 1% of the first frequency above. The other frequency is separated from the first by the frequency ζ and may correspond to more complex orbits on the network. A second-harmonic manifold is also observed. The close agreement of the giant-orbit frequency as well as the frequencies observed in the linear-chain case of Fig. 6 with the relevant frequency assignments of Graebner strongly support both the qualitative and quantitative aspects of this Fermi-surface model.

ACKNOWLEDGMENTS

The authors wish to thank J. E. Graebner and L. F. Mattheiss for many stimulating discussions. In addition they wish to thank J. E. Graebner for his help with the Fast Fourier Transform programs used in analyzing our oscillatory data.

*Now retired.

¹J. E. Graebner and W. D. Ryden, *Bull. Am. Phys. Soc.* **15**, 312 (1970); and J. E. Graebner (unpublished).

²L. F. Mattheiss (unpublished).

³E. Fawcett, *Advan. Phys.* **13**, 139 (1964); and R. W. Stark and L. M. Falicov, *Progress in Low Temperature Physics*, edited by C. J. Gorter (Wiley, New York, 1967).

⁴G. F. Brennert, W. A. Reed, and E. Fawcett, *Rev. Sci. Instr.* **36**, 1267 (1965).

⁵L. F. Mattheiss (private communication).

⁶W. D. Ryden, W. A. Reed, and E. S. Greiner, *Bull. Am. Phys. Soc.* **16**, 337 (1971).

⁷W. D. Ryden, W. A. Reed, and E. S. Greiner (unpublished).